This is a preprint, the final version is subject to change, of the American Mineralogist (MSA)
Cite as Authors (Year) Title. American Mineralogist, in press.
(DOI will not work until issue is live.) DOI: http://dx.doi.org/10.2138/am-2016-5475

Redox states of uranium s

in samples of microlite and monazite

Elena V. Puchkova [1], Roman V. Bogdanov [1], and Reto Gieré [2]

[1] *St. Petersburg State University, 199034, St. Petersburg, Russia (e-mail: bogdanov@RB7584.spb.edu)*

[2] *Department of Earth and Environmental Science, University of Pennsylvania, Philadelphia, PA 19104-6316, USA (e-mail: giere@sas.upenn.edu)*

ABSTRACT

By applying the method of chemical shifts of the uranium $L\alpha_1$ and $L\beta_1$ X-ray emission lines, the oxidation state of U has been determined in select samples of microlite and monazite. From the relative contents of U^{4+}, U^{5+} and U^{6+} species, the oxygen coefficients have been calculated as a characteristic of U-oxidation rate. It is shown that the oxidation state of U is higher in the studied microlite than in monazite. Possible mechanisms of U oxidation in these two types of minerals are discussed, and it appears that the crystal structure of monazite plays an important role in stabilizing the U redox state. Spontaneous purification of the monazite structure from alien atoms, including U, may be possible via recrystallization of the alpha-recoil tracks. An explanation is suggested for intensive U oxidation in microlite and in other minerals of the pyrochlore group.

Keywords: microlite, monazite, oxidation states of uranium, chemical shifts of X-ray lines, metamict state, spontaneous recrystallization.

INTRODUCTION

Uranium- and Th-containing minerals are regarded as natural analogues of matrices to be used for the immobilization of actinides. Among the phases that have been studied in this respect, the most common ones are titanates, Ti-Ta-niobates, phosphates, silicates, and silico-phosphates of groups II, XIII and XIV in the Periodic Table of the Elements. In particular, crystalline pyrochlore ceramics are since several decades at the center of attention of researchers as possible waste forms for the immobilization of excess weapons-grade plutonium and other actinides (Lumpkin et al., 1986, 1999, 2014; Lumpkin and Ewing, 1988; Buck et al., 1999; Icenhower et al., 2000; Gieré et al., 2000, 2002; Lumpkin, 2001; Stefanovsky et al., 2004; Zhang et al., 2013). One of the most important goals of such research is to try to forecast the long-term behavior of these ceramic waste forms under conditions of an underground repository. Most of the minerals mentioned above would be rendered metamict as a result of the gradual accumulation of alpha-recoil collision cascades, as documented by numerous X-ray and electron diffraction studies (see e.g., Lumpkin et al., 2014). These and other investigations provided a vast amount of data on the structure of metamict minerals, i.e., on dislocations in, and damages to, the atomic arrangement within the solid. At the same time, however, not enough data are available on the electronic disorder observed in metamict minerals (e.g., Hawthorne et al., 1991; Salje et al., 2011). This discrepancy, thus, results in a relative lack in knowledge of the relationship between the chemical composition and the physico-chemical, colloid-chemical, nuclear-chemical and radiation-chemical processes occurring in complex compositions of amorphous and crystalline materials.

Possible approaches to studying this specific aspect of solid-state chemistry include the examination of chemical and redox states of polyvalent elements present in these complex

natural systems as well as the investigation of how these states may be modified by external processes. In addition to providing important fundamental knowledge, studies of *d*- and *f*-elements in minerals as well as reconstructions of the physical and chemical processes that occurred throughout the geological history of these minerals could help in predicting the behavior of host phases for nuclear waste in deep geological formations. Important data on the state of U, Pb and Fe in various minerals were published, for example, by Zhang et al. (2002, 2003), Kramers et al. (2009), and Salje et al. (2011).

The main goal of the present work is to report data for the oxidation state of uranium in select specimens of microlite and monazite, both minerals that are considered to be natural analogues of host phases for the immobilization of actinides in high-level waste (HLW). In addition, this paper explores possible explanations for the different results obtained for monazite and microlite.

MATERIALS AND METHODS

Sample description

Microlite belongs to the pyrochlore-supergroup minerals, which crystallize in the isometric crystal system (space group $Fd\bar{3}m$ or its subgroups; $a \approx 10.4$ Å; $Z = 8$) and conform to the general formula $A_{2-m}B_2X_{6-w}Y_{1-n}$. In this formula, *A* and *B* represent 8- and 6-coordinated cation sites, respectively and *X* and *Y* are 4-coordinated anion sites (e.g., Atencio et al., 2010). The general microlite formula is $(Ca,Na)_2Ta_2O_6(O,OH,F)$.

The studied microlite originates from a Li-rich pegmatite in the Mutala area, Alto Ligonha, Mozambique (Gieré et al., 2000). The sample investigated here is a piece of a large crystal and its two smaller fragments, which were first examined visually with the aid of a binocular (10x60) microscope. There are few small particles (0.2 – 1 mm) formed on the surface of the broken-up crystal. The microlite crystals are slightly unusual, as they are evidently not octahedral, but rather show some dodecahedron faces. Overall, they exhibit a yellowish-grey color, but the outer layers of the large fragment are dull brown, probably because of the strong chemical zoning observed in microlite from this locality (Gieré et al., 2000). Along cracks and parallel to the crystal faces of microlite, one can observe light-colored mica (muscovite or lepidolite), which possibly resulted through epitactic growth. The content of mica in the studied sample is only 1-2 vol.%. Along the cracks (but not on the surface), inclusions of a fine-grained, soft aggregate of white or light cream color can be seen (sericite or kaolinite). The content of these inclusions is also small (< 2 vol.%). In addition, microlite also hosts minute quantities of very small grains of a dark brown mineral with an oblong shape, most likely bismutite, a mineral identified as inclusions in microlite from this locality (Gieré et al., 2001).

The overall U content in the studied microlite sample is 1.3 ± 0.1 wt.%, as determined by the method of chemical shifts of X-ray emission lines (see below). The sample exhibits a low level of radioactivity (23-25 μR/h), as determined with an SPR radiometer. For comparison, the natural background in our laboratory in St. Petersburg is 18-20 μR/h.

To carry out the instrumental X-ray studies, the following procedure of sample preparation was performed: First, the sample was crushed and the resulting powder was separated into two granulometric fractions: *microlite 1* (<0.25 mm) and *microlite 2* (0.25-0.5 mm). Both fractions

were checked for the presence of magnetic components, which however, were present only in minute quantities. After removal of these magnetic components, the non-magnetic fraction was purified in a heavy liquid (bromoform), yielding only a very small quantity of the light fraction. However, some mica and other impurities contained in microlite were entrained into the heavy mineral concentrate, but their amount was < 5% of the total sample mass.

Two monazite samples were also investigated in order to be able to compare with the data obtained for microlite. Monazite (monoclinic) ideally has the composition $LnPO_4$, with *Ln* = La, Ce, Pr, and Nd. It may contain smaller amounts of Sm-Lu and Y, and typically exhibits extensive solid solution toward other end-members with Ca, Th, and U on the *Ln* site. Monazite was chosen as reference sample because it is considered to be a suitable host phase for the immobilization of actinides (Lutze and Ewing, 1988; Meldrum et al., 1998; Volkov, 1999; Orlova et al., 2006; Schlenz et al., 2013; Lumpkin et al., 2014).

The two samples of monazite studied here also originated from pegmatites: *monazite 1* from a pegmatite in the Chupa area of northern Karelia, Russia; and *monazite 2* (with noticeable veinlets of uranium dioxide) from a pegmatite in China. The contents of U and Th in *monazite 1* are 0.4±0.1 wt.% and 2.5±0.1 wt.%, respectively. *Monazite 2* contains U in amounts that are comparable with those in microlite, but it also hosts up to 8 wt.% Th.

To carry out the instrumental X-ray studies of the monazites, the same sample preparation was performed as that used for microlite (see above).

Determination of uranium redox states

The U oxidation states in the minerals were studied by using the method of chemical shifts of the $L\alpha_1$ and $L\beta_1$ X-ray emission lines (Bogdanov et al., 1999; Batrakov et al., 2000). Measurements were carried out with a 2 m-long single-crystal spectrometer (originally designed by O. I. Sumbaev) with Cochois focusing. The monochromator was a cylindrically curved (r = 2000 mm), 0.3 mm-thick quartz crystal. Fluorescence of the samples was excited by a combination of Bremsstrahlung and characteristic radiation emitted by the silver anode of an X-ray tube (I = 46 mA, U = 47 kV) and recorded with a NaI(Tl) crystal-based scintillation detector.

Line intensities were measured at each point successively for all the samples by subjecting them alternately to the primary beam. To compensate for the aberration shift due to the geometrically non-equivalent location of the samples, the chemical shifts δ of the $L\alpha_1$ and $L\beta_1$ X-ray emission lines of uranium (δU-$L\alpha_1$ and δU-$L\beta_1$) were measured at two equivalent positions of the detector and monochromator relative to the incident beam. The chemical shifts thus measured were averaged. Line profiles were approximated by Gaussian-Lorentzian functions, and their shift δ was determined from changes in the line position at the inflection point relative to the corresponding values for the uranium line in $UO_{2.00}$.

The content of different U species was calculated according to the procedures described in detail by Bogdanov et al. (1999) and Batrakov et al. (2000). Briefly, these calculations are performed on the basis of the two-dimensional δU-$L\alpha_1$ *vs.* δU-$L\beta_1$ correlation diagram shown in Fig. 1, where

$$U(VI) = \frac{d_3}{d_3 + d_4}; \qquad (1)$$

$$(2)$$

$$U(V) = \frac{d_1}{d_1 + d_2} \times \frac{d_4}{d_3 + d_4};$$

$$U(IV) = \frac{d_2}{d_1 + d_2} \times \frac{d_4}{d_3 + d_4}. \quad (3)$$

Segments d_1 to d_4 are determined from the numerical values of Z and Y in the coordinate system used (Z = δU-$L\alpha_1$; Y = δU-$L\beta_1$) and from the coordinates of the corners of the triangle shown in Fig. 1:

$$d_1 = [(Z_4 - Z_1)^2 + (Y_4 - Y_1)^2]^{1/2}; \quad (4)$$

$$d_2 = [(Z_2 - Z_4)^2 + (Y_2 - Y_4)^2]^{1/2}; \quad (5)$$

$$d_3 = [(Z_4 - Z_0)^2 + (Y_4 - Y_0)^2]^{1/2}; \quad (6)$$

$$d_4 = [(Z_3 - Z_0)^2 + (Y_3 - Y_0)^2]^{1/2}, \quad (7)$$

where: (Z_0, Y_0) are the coordinates of the studied substance (filled square); (Z_1, Y_1), (Z_2, Y_2), and (Z_3, Y_3) are the coordinates of the three reference uranium oxides UO_2, U_2O_5, and UO_3, respectively; (Z_4, Y_4) are the coordinates of the intersection point (open circle) between the lines defined by (Z_0, Y_0) − (Z_3, Y_3) and (Z_1, Y_1) − (Z_2, Y_2), whereby Y_4 and Z_4 are determined as follows:

$$Y_4 = \frac{72 \times (152Y_0 + 97Z_0)}{101 \times (97 - Y_0) + 72 \times (Z_0 + 152)}, \quad (8)$$

$$Z_4 = \frac{101 \times (152Y_0 + 97Z_0)}{101 \times (97 - Y_0) + 72 \times (Z_0 + 152)}. \quad (9)$$

If the contents of U^{4+}, U^{5+} and U^{6+} are known, the overall *oxygen coefficient* of uranium ($2+X$) in a sample can be calculated from the following relation:

$$(2+X) = U^{4+} \times 2.0 + U^{5+} \times 2.5 + U^{6+} \times 3.0. \quad (10)$$

The oxygen coefficient provides a measure of the tendency of U to be oxidized in the mineral.

RESULTS AND DISCUSSION

Results of our X-ray spectral investigation of microlite and monazite are presented in Table 1, which in addition to the chemical shifts δ in the U-$L\alpha_1$ and U-$L\beta_1$ lines also lists the magnetic broadening ($\Delta\Gamma$) of these lines relative to UO_2. The line broadening is related to the effect of interatomic redistribution of the spin density on the split $5f_+$ and $5f_-$ levels of uranium, and it provides information on a spin constituent of the chemical shift (Krivitsky et al., 2004). Table 1 further displays the values of overall oxygen coefficients calculated according to equation (10) from the relative content of U species.

As expected, the overall oxygen coefficients in both samples of microlite are very similar, being practically identical within experimental error (see δ values in Table 1). The slightly higher U^{6+} content in *microlite 1* (< 0.25 mm granulometric fraction) compared to *microlite 2* (0.25-0.5 mm) might be explained by oxidation in the atmosphere of some of the U^{5+} in the finest particles. Despite the relatively low U content in the studied microlite as compared with other minerals of the pyrochlore supergroup, a substantial oxidation of U is observed: approximately 2/3 of the initial U^{4+} have been converted into pentavalent and hexavalent states.

In contrast, only ~26% of the initial U^{4+} have been oxidized in the studied monazite samples (Table 1).

Do the oxygen coefficients correlate with geological age?

The age of *monazite 1* is between 1.76 and 1.93 Ga (Avdzeyko, 1955; Tugarinov et al., 1974). Using this age and the half-life of ^{238}U (4.468 Ga), the fraction of decayed ^{238}U is calculated at 0.239-0.259. The analytical results for the different redox species of U in this monazite (Table 1) allow for calculation of the oxygen coefficient according to equation (10), yielding a value of 2.244. This value corresponds to an *oxygen index* (X) of 0.244, which means that the oxygen coefficient of U increased by X from its initial value of 2.000 (all U assumed to be U^{4+} originally). The age of *monazite 2* is 1.00±0.05 Ga (A.S. Sergeev, personal communication), yielding a fraction of decayed ^{238}U of 0.137-0.150; the oxygen coefficient calculated from the redox data given in Table 1 is 2.149, i.e. $X = 0.149$. Thus, as a first approximation, the values of X in both monazite samples are very similar to those of the fraction of decayed ^{238}U.

The age of the studied microlite is approximately 440 my (chemical age determination; see Gieré et al., 2000), which yields a value of 0.066 for the fraction of decayed ^{238}U. With the redox data obtained for the two samples (Table 1), oxygen coefficients of 2.570 (microlite 1) and 2.550 (microlite 2) can be calculated. The associated values for X (0.570 and 0.550, respectively) are, thus, considerably higher than the fraction of decayed ^{238}U.

Therefore, our data suggest that the mechanisms and efficiency of U oxidation in monazite and microlite are substantially different, whereby the U-oxidation *rate* in microlite appears to be higher than in the two monazites.

Let us try to understand the reason for these differences. The fact that the value of *X* in our monazite samples is close to the fraction of decayed ^{238}U may be interpreted to indicate that self-oxidation of U in monazite is mainly the result of the following, combined nuclear-chemical mechanism:

$$2\ U^{4+}O_2 \rightarrow PbO + U^{6+}O_3. \qquad (11)$$

This mechanism would lead to oxidation of one U^{4+} atom for every single ^{238}U that decays to ^{206}Pb. In microlite, however, it appears, that apart from the effect of oxygen, several additional radiation- and chemistry-related factors influence the redox state of U atoms. These additional mechanisms are not realized, or not sufficiently effective, in the monazite samples studied here.

Evidence for low efficiency of radiation mechanisms in monazite

By using the chemical shifts method, Bogdanov et al. (2002b) investigated the oxidation state of Ce in four monazites of different origin and age, as well as in the complex minerals aeschynite $[(Y,Ca,Fe,Th)(Ti,Nb)_2(O,OH)_6]$ and britholite $[Ca_2(Ce,Ca)_3(SiO_4,PO_4)_3(OH,F)]$. In three of the monazites (samples #8, 9, 11), cerium was found to have remained in its initial trivalent state, whereas in the fourth monazite (sample #10), Ce^{4+} was present, but its content did not exceed 1-2 % of the total Ce. On the contrary, in aeschynite and, especially, in the two studied britholite samples, up to 35% of the Ce was present as Ce^{4+}. It is important to note here that upon heating, the Ce^{4+} fraction in britholite decreased, whereas in aeschynite the Ce^{4+} disappeared completely (Bogdanov et al., 2002b). Thus, in contrast to the silico-phosphate britholite and the Ti-Ta-

niobate aeschynite, cerium in monazite appears to be more resistant to oxidation through self-irradiation, thus preserving its initial trivalent oxidation state.

Therefore, radiation should undoubtedly be considered an effective agent for this oxidation, in addition to the self-oxidation mechanism described by reaction (11). It can cause both ionization of Ce and destruction of the crystalline structure of most radioactive minerals. However, ionization is an indispensable, though not always sufficient, condition for the oxidation of Ce. The point is that, upon oxidation of a Ce^{3+} ion, the second *f*-electron is involved in the formation of a chemical bond, which results in a change of spatial orientation of the chemical bonds of Ce. However, it is only the Ce^{4+} phosphate $Me(II)_{0.5}Ce_2(PO_4)_3$ (Orlova et al., 2006) that is isostructural with monazite, and this phase does not correspond to the composition of the initial monazite, its formation through recrystallization of damaged crystal zones in recoil tracks being impossible. In other words, the involvement of the second *f*-electron of Ce is not compatible with the geometry of the monazite crystal structure. The new steric orientation of chemical bonds caused by Ce^{4+} can be stable only in the new amorphized structure of britholite and aeschynite.

Using infrared spectroscopy, Zhang et al. (2002, 2003) identified a complex behavior of the various redox forms of U in metamict and annealed zircon: they have shown that U ions in metamict zircon can be assigned to two categories with different structural environments: 1) U ions in the remaining crystalline regions ($U^{4+}_{crystal}$ and $U^{5+}_{crystal}$); and 2) U ions in the amorphous regions ($U_{amorphous}$, mainly tetravalent). They also reported that the ratio of $U^{4+}_{crystal}/U^{5+}_{crystal}$ in the crystalline domains increased with increasing metamictization. These observations led the authors to conclude that the tetravalent state is the preferable oxidation state of U in radiation-

241 damaged zircon. The increase in $U^{4+}_{crystal}/U^{5+}_{crystal}$ with increasing metamictization can be
242 explained as due to trapping of electrons by the U^{5+} ions. Heating released the trapped electron,
243 which thus decreased $U^{4+}_{crystal}/U^{5+}_{crystal}$. The increase in $U^{4+}_{crystal}/U^{5+}_{crystal}$ with increasing
244 metamictization could also result from a radiation-induced change of local structures, which
245 could lead to modifications of the local configurations associated with Zr^{4+} and Si^{4+} sites (Zhang
246 et al., 2002; 2003).

247 It is reasonable to assume a certain relationship between the oxidation state of an atom and
248 the symmetry of its nearest polyhedron. The work of Salje et al. (2011), however, does not
249 confirm such an assumption. Using ^{57}Fe Mössbauer spectroscopy, these authors found that iron
250 in metamict titanite is partitioned between amorphous and crystalline regions according to its
251 valence: Fe^{3+} exists in the crystalline titanite matrix, whereas Fe^{2+} occurs almost exclusively in
252 regions that are amorphous due to radiation damage. Both valence forms are located in the Ti
253 positions. The Mössbauer spectra for both oxidation states of Fe are well defined, resembling
254 those found in a fully crystalline matrix. The authors concluded that the local structure of the
255 amorphized regions exhibits a high degree of short-range order, and that the local environment of
256 Fe (and hence Ti) is similar to that found in the crystalline titanite structure. If this is indeed
257 correct, it remains to be explained why Fe^{2+} is stabilized in amorphized zones.

258

259 **Do U^{5+} and U^{6+} exist in the monazite structure?**

260 Since monazite retains its crystal structure under the effects of radiation, the possibility of
261 uranium atoms existing in monazite in the U^{5+} and U^{6+} states needs to be discussed. According to
262 Batrakov et al. (2004) and Krivitsky et al. (2004), the transition from UO_2 to $UO_{2.5}$ involves 0.18
263 of the electron density of a 5*f*-electron and 0.02 of that of a 6*d*-electron in the chemical bond.

Upon oxidation of UO_2 to UO_3, the fractions of the 5*f*- and 6*d*-electrons increase to 0.25 and 0.28, respectively. Moreover, no less than 1.10 of the electron density of the 5*f*-electron participates in the interatomic redistribution of electron and spin density on the split $5f_+$ and $5f_-$ levels of U when its valence increases from +4 to +6. Changes in the nature and spatial orientation of chemical bonding violate conditions of even a limited isomorphism of U^{4+} in the crystal structure of monazite. As a consequence, upon recrystallization of amorphized regions formed by recoil atoms, the crystal structure of monazite may reject those U atoms whose radial distribution of the electron density or spatial orientation of hybrid orbitals do not suit the geometry of the surrounding lattice.

This process is analogous to the purification of substances by the method of zone recrystallization and is readily observed in polymorphic phase transformations (first- and second-order phase transitions). The behavior of radiogenic ^{113m}In atoms in metallic Sn may serve as an example (Alekseev et al., 1998a): upon transition from the tetragonal to the rhombic modification of Sn at 200 ºC, radioactive atoms of In from the bulk of a Sn foil move up to its surface. In addition, up to 20% of the In atoms are found in the gaseous phase, which does not contain any Sn atoms. An analogous ejection of foreign atoms upon polymorphic transformation was observed in Mo and W (Alekseev et al., 1998b, 2002), as well as in a number of other substances.

It is most probable that the U atoms, which were rejected by the crystal structure of monazite, could diffuse to other sites, where they accumulate and form oxide phases of their own, e.g. in pores, cracks, along grain boundaries, or in the vicinity of dislocations. Such diffusion can be intensified by radiation, in particular, by the energy dissipation of recoil atoms during elastic tangential collisions with other atoms. High mobility of Pb, Th, and U atoms as

287 well as the possibility of their removal from monazite upon exposure to low temperatures have
288 been repeatedly observed in monazites, and this mobility is greater than the one corresponding to
289 the volume diffusion coefficients of these elements (Cherniak and Pyle, 2008; Olander and Eyal,
290 1990). Seydoux-Guillaume et al. (2012) underlined the important role of radiation damage
291 effects, in particular swelling-induced fracturing, and the essential role of porosity and cracks in
292 the migration processes within monazites.

293 It has been noted repeatedly that U-rich zones occurring in various minerals are also
294 enriched in accessory minerals. For example, microradiography revealed that U is evenly
295 distributed in optically transparent and pure zircon crystals, whereas high U concentrations
296 occurred locally, e.g. along cracks and in roiled and less transparent parts of the mineral, which
297 would suggest that part of the U has been segregated into micro-inclusions of accessory U
298 minerals (Komarov, 1977; Komarov et al., 1980, 1985; Tsimbal et al., 1986). These conclusions
299 may be applied to monazites as well: the presence of uraninite inclusions in the two monazite
300 samples studied here has indeed been proven, i.e., by using X-ray diffraction for monazite 1
301 (sample from Karelia), and by detailed optical microscopy combined with immersion liquids for
302 monazite 2 (sample from China). Similarly, the association of uraninite and monazite has been
303 reported previously from other occurrences (e.g., Bogdanov et al., 1999; Bogdanov et al.,
304 2002b).

305 Undoubtedly, the primary separation mechanism of isomorphic and non-isomorphic U
306 species in minerals is connected with the primary crystallization from a melt or fluid and with the
307 accessory-mineral growth. Uranium, the content of which exceeds the isomorphic capacity of the
308 mineral under particular physical and chemical conditions, is rejected by the front of the growing
309 crystal and is trapped by it later as U-rich micro-inclusions (Vorobiev, 1990). Micro-crystals of

uraninite in monazite, however, might also be formed upon cooling through exsolution from an originally U-rich monazite. These mechanisms, however, are most probably not the only ones possible, as indicated by various investigations (e.g., Olander and Eyal, 1990; Seydoux-Guillaume et al., 2012). Komarov (1977) suggested, for example, that redistribution of U in the mineral association occurred after the formation of crystals by a partial recrystallization of U-containing minerals. We propose that post-crystallization alteration, especially the recrystallization of the amorphized substance in recoil tracks, is another very likely mechanism that leads to the rejection of U from the monazite structure upon recrystallization. This process would lead to the decomposition of single-phase mineral structures and could take place during long-term storage of actinide host phases. Similar post-crystallization alteration features have also been reported for metamict microlite, e.g., from Mozambique (Gieré et al., 2001) and from the Kola Peninsula (Kudryashov et al., 2015).

An alternative or, perhaps, complementary mechanism of preserving U^{4+} in the structure of monazite could be radiation-and-chemical reduction of U, i.e., electron capturing by penta- and hexavalent U atoms. It must be assumed that the relatively rapid recrystallization within the recoil tracks normalizes the process of electron transfer in the conduction band of the mineral. The consequence of this is neutralization of the excess charge of uranium atoms, like the reduction process $Ce^{4+} \rightarrow Ce^{3+}$. The same mechanism may be effective for the reduction of other polyvalent impurities in monazite.

Incorporation of U^{4+} in monazite during recrystallization of recoil tracks?

The next issue to be discussed is whether or not the crystal structure of monazite could assimilate those tetravalent U atoms, which happened to lie within the recoil track at the moment of

recrystallization of the damaged structure. The answer does not seem evident: upon formation of primary accessory minerals in pegmatite dikes, U^{4+} atoms are incorporated at high temperatures (e.g., via heterovalent compensation isomorphism), when the difference in ionic radii is leveled by the large amplitude of atom oscillation. Based on the radiochemical data available, however, it can be assumed that some of the U^{4+} is incorporated into the structure of monazite even at low temperature, during recrystallization of amorphous parts.

The effect of assimilation is revealed upon the incongruent dissolution of monazites, as well as of xenotime, in solutions of strong hydrochloric acid. Results of the action of 6 molar HCl solutions (with and without reducing agents added) on these minerals (Avenirova et al. 1992) are given in Table 2. The data show that the radioactivity of ^{238}U in the leachates is higher than that of ^{234}U, whereby the deficit of the radiogenic uranium is observed in both U^{4+} and U^{6+} species. This result cannot be explained on the basis of a single-phase model for these samples. Therefore, we conclude that the $^{234}Th(^{234}U)$ recoil atoms penetrate from the outer layer of the phase, which is richer in U than the bulk monazite (i.e., from the UO_{2+X} phase present in the mineral association), into the structure of monazite (or xenotime), where they are fixed upon spontaneous recrystallization within the recoil track. Here we come across a variant of the effect observed by Chalov (1975) and Shirvington (1983), namely that the leaching solutions are enriched in the parent U isotope rather than the radiogenic isotope. On average, the fraction of U going into solution is 10-20%, and is mainly tetravalent (Avenirova et al., 1992).

The explanation suggested here for the observed isotopic effects of the incongruent dissolution of monazite seems to be the only one possible, but it leads to a paradoxical conclusion: since a substantial part of U in the monazite and xenotime is present in the uranium oxide phase, it means that all our arguments on the mechanism of U oxidation in monazites are

related not only to the original monazite, but equally to the uraninite. At the same time, this conclusion is not surprising, since both uraninite and monazite share the property of preserving their crystal structure, as the alpha-recoil tracks have relatively short life times (1-4 x 10^4 y; Eyal and Fleischer, 1985a, 1985b). The other common property of uraninite and monazite is the tendency to eject foreign atoms, or atoms of different valence to the periphery of crystal grains. Already more than thirty years ago, Dubinchuk and Sidorenko (1978) observed that the radiogenic Pb in only slightly oxidized samples of uraninite was not only located as PbO on intergrain surfaces, but that it also occurred as a distinct, metallic Pb phase, which was present as either rounded aggregates or as tiny squares (0.2-0.5 μm across). These authors have further described that in fairly strongly oxidized samples of uraninite, hexavalent U was rejected from the structure, which led to the formation of lead uranate ($PbUO_4$).

It is quite understandable why Pb is not stabilized in the UO_2 structure: the laminated tetragonal and chain-like rhombic crystal lattices of the red and yellow PbO do not match the face-centered cubic fluorite UO_2 lattice. A mismatch of the symmetry of the chemical bonds and the geometry of the surrounding lattice should be understood as a non-optimal spatial overlap of electron clouds of the central atom and anions in the coordination polyhedron. It is the weak chemical bond with the surrounding structure that apparently determines the effect of rejection of Pb atoms from the regular lattice upon recrystallization of recoil tracks.

Thus, the apparent monazite is a combination of monazite and uraninite, which are both resistant to radiation damage, and thus metamictization, and which mutually complement each other for the balance of redox states to be accounted for.

Oxidation of U in microlite

379 In contrast to monazite, microlite is subject to significant oxidation (see above), which results in
380 the fraction of oxidized U in the mineral exceeding the fraction that is typical for closed
381 uranium-oxide systems. Apparently, it concerns all Ti-Ta-niobates of the pyrochlore group, as
382 indicated by results from another study that applied the chemical shifts method (Bogdanov et al.,
383 2002a): a sample of U-rich pyrochlore from a granite pegmatite in the Vuori-yarvy Massif,
384 northwestern Karelia (Russia) contained 20% U^{4+}, 37% U^{5+}, and 43% U^{6+}. These values
385 correspond to an oxygen coefficient of 2.615. Since the age of this specimen is 1.74 Ga, the
386 fraction of decayed U is only 0.24 of its initial amount and, consequently, by analogy with
387 monazite, the corresponding oxygen coefficient should be equal to 2.24. In two other U-rich
388 pyrochlore samples, a 0.25 Ga old sample from quartz veins of alkaline pegmatites in the Urals
389 and a 0.52 Ga old specimen from metasomatites in the Chupa area of northern Karelia (Russia),
390 all U was found to be hexavalent, but it did not occur as oxide species, but rather as the uranyl
391 (UO_2^{2+}) species.

392 It may be concluded that there are at least two factors that determine the chemical and
393 redox states of U in these minerals: First, a low resistance of the corresponding structures
394 towards metamictization. Because oxidation is associated with a change of the nature and
395 symmetry of chemical bonds of atoms with their environment, this process most easily occurs in
396 metamict structures, where there are no crystallographic limitations for the new redox state to be
397 realized. Moreover, it concerns such species as uranyl ions, which are not capable of isomorphic
398 substitution of atoms in accessory minerals. An exception can be made for the cubic lattice of
399 uraninite, which remains unchanged for oxygen coefficient values up to 2.25. It is well known
400 that there is a sharp decrease in the U-oxide density when the oxygen coefficient increases to
401 values > 2.4 (Weigel, 1986). This is assumed to be caused by the appearance in the structure of

U oxide with uranyl-type bonds, the two short collinear U–O main bonds being formed in a combination with 4-6 less strong bonds lying in the plane that is approximately perpendicular to the two first bonds. Yet, the appearance of uranyl-type bonds does not imply the compulsory formation of isolated uranyl groups. It is suggested, that the highest oxidation states of U (V, VI) in uranium oxides, as well as in most of the known oxide compounds of actinides, are stabilized owing to the formation of uranyl (actinyl)-type bonds, thereby preserving homogeneity of the system. It should be noted that the accumulation of oxidized species of atoms in uraninite will ultimately lead to the cubic lattice being transformed into the rhombic one. Hence, it is clear that metamictization of the mineral that hosts U or other actinides does remove crystallographic (steric) limitations for changes resulting from both radiation-chemical and nuclear-chemical processes.

The second factor, which can dramatically influence the chemical state of U in minerals of the pyrochlore group, is the presence of crystallization and constitutional water. This water, in combination with the radiation process, can initiate a chain of oxidation–reduction reactions. For example, the formation of hydronium in pyrochlore can be the result of the following processes:

$$2\ OH^- + He^{2+}\ (\alpha) \rightarrow 2\ OH^0 + He^0 \qquad (12)$$

$$U^{4+} + 2\ OH^0 \rightarrow UO_2^{2+} + 2\ H^+ \qquad (13)$$

$$H^+ + H_2O \rightarrow H_3O^+. \qquad (14)$$

There are other possible variants for radiation-chemical reactions in Ti-Ta-niobates: for example, radiation creates traps to capture electrons and holes of various depths, which determine the chemical state of atoms in the mineral.

In connection with this, the following problems are of interest: how pronounced is the difference between the synthetic phase and its natural analogue? To what extent may these differences be neglected or, vice versa, how can they be accounted for when analyzing results of other studies? To what extent is the prognostic information correct in regard to the long-term behavior of HLW hosts when studying natural analogues?

IMPLICATIONS

Knowledge of the redox state of uranium is of interest for two reasons: firstly, it yields information about the nuclear-chemical and radiation-chemical processes taking place in radioactive minerals over geological timescales, and secondly, it provides a basis for the long-term prediction of the chemical state of actinides in potential host phases for high-level nuclear waste. Our study has shown that in the monazite samples, 74% of the U is still tetravalent, in spite of their considerable geological age, whereas only ~33% of the U remains in its tetravalent state in the much younger microlite. These results demonstrate that the mechanism of U oxidation is very different for the two minerals: it is largely due to a nuclear-chemical process in monazite (reaction 11), whereas in the more intensely oxidized microlite it is also due to a radiation-chemical mechanism, which results from metamictization.

We also conclude that upon recrystallization of the amorphized regions in monazite, the crystal structure rejects the penta- and hexavalent U atoms, which then form separate U oxide phases. Such processes, therefore, can lead to a transformation of a monophase host into a multiphase assemblage with different properties (e.g. chemical durability). The similarity of nuclear waste form materials with their naturally occurring analogues may thus be quite limited,

except if the chemical compositions of the mineral and the synthetic matrix material closely coincide. For example, a study of fergusonite from a granite pegmatite showed the ability of the mineral to retain U even in the completely metamict structure (Gieré et al., 2009). The authors concluded that fergusonite could be a phase suitable to be included in ceramics designed for the immobilization of HLW. This situation, however, demands further clarification, as illustrated by the following example: during their study of pyrochlore-based ceramic waste forms, Strachan et al. (2005) observed that despite amorphization of the material at high alpha-decay doses, there was no cracking and no effect on the kinetics of ceramic dissolution. The authors concluded on the basis of structural changes resulting from alpha-decay of incorporated ^{238}Pu that even though pyrochlore is susceptible to radiation-induced damage, it remained chemically and physically viable as a material for immobilizing surplus weapons-grade plutonium. In contrast to these results, Bogdanov et al. (2002a) observed high uranium leach rates in their study of natural pyrochlores; they ascribed this extensive leaching to the presence of all U in the uranyl form $(UO_2)^{2-}$, which resulted from radiation-chemical reactions, presumably taking place in the presence of an aqueous phase. This example, thus, demonstrates that analogies between a mineral and its corresponding mineral-like phase in HLW waste forms, can only be established if several conditions and processes are similar, e.g., chemical composition, self-irradiation and aqueous alteration. Otherwise, the immobilization characteristics of HLW matrices determined in the laboratory have, unfortunately, limited predictive character.

ACKNOWLEDGMENTS

The authors are grateful to two anonymous reviewers and to Peter Burns and Keith Putirka for their valuable suggestions and critical remarks, which have helped us in improving the manuscript.

REFERENCES CITED

Alekseev, I.E., and Antropov, A.E. (2002) Accelerated transfer of ^{99m}Tc admixture atoms on polymorphic transformation in irradiated metal molybdenum (*in Russian*) Radiokhimia, 44/4, 334-336.

Alekseev, I.E., Bondarevsky, S.I., and Yeryomin, V.V. (1998a) Specificity of physico-chemical behavior of "hot" admixture atoms on phase transitions in metals I. Behavior of admixture indium atoms in metal tin (*in Russian*). Radiokhimia, 40/5, 427-432.

Alekseev, I.E., Bondarevsky, S.I., and Yeryomin, V.V. (1998b) Specificity of physico-chemical behavior of "hot" admixture atoms on phase transitions in metals II. Behavior of admixture rhenium atoms in metal tungsten (*in Russian*). Radiokimia, 40/5, 440-443.

Atencio, D., Andrade, M.B., Christy, A.G., Gieré, R., and Kartashov, P.M. (2010) The pyrochlore supergroup of minerals: nomenclature. Canadian Mineralogist, 48, 673-698.

Avdzeyko, G.V. (1955) The role of isotopic analysis in the determination of age. Proceedings of the 3rd session of the commission to determine the absolute age of geological formations (*in Russian*). USSR Academy of Sciences, Moscow, 153-162.

Avenirova, L.V., Bogdanov, R.V., Ozernaya, S. A., and Sergeev, A.S. (1992) Chemical consequences of nuclear transformations in minerals. 2. Behavior of U-234 and U-238 on incongruent dissolution of natural monazite and orthite (*in Russian*). Radiokhimia, 34/3, 200-213.

Batrakov, Yu.F., Bogdanov, R.V., Puchkova, E.V., and Sergeev, A.S. (2000) Identification of the uranium state in minerals by the chemical shift of hard X-ray lines. Radiochemistry, 42/2, 112-118 (Translated from Radiokhimiya, 2000, 42/2, 106-112).

Batrakov, Yu.F., Krivitsky, A.G., and Puchkova, E. V. (2004) Relativistic component of chemical shift of uranium X-ray emission lines. Spectrochimica Acta. Part B: Atomic Spectroscopy, 59, 345-351.

Bogdanov, R.V., Batrakov, Yu.F., Puchkova, E.V., and Sergeev, A. S. (1999) "Programme of Natural Analogues Studies" and identification of the chemical state of uranium in natural substances. Radiochemistry, 41/5, 409-433 (Translated from Radiokhimiya, 1999, 41/5, 385-408.

Bogdanov, R.V., Batrakov, Yu F., Puchkova, E.V., Sergeev, A.S., and Burakov, B.E. (2002a) Study of natural minerals of U-pyrochlore type structure as analogues of plutonium ceramic waste form. Materials Research Society, Symposium Proceedings, 713, 295-301.

Bogdanov, R.V., Zaytsev, Y.M., and Sergeev, A.S. (2002b) The use of cerium valence state for evaluation of accessory minerals durability to radiation damage. Materials Research Society, Symposium Proceedings, 713, 469-476.

Buck, E.C., Chamberlain, D.B., and Gieré, R. (1999) Intergrowth structures in synthetic pyrochlores: Implications for radiation damage effects and waste form formulation. Materials Research Society, Symposium Proceedings, 556, 19-26.

514 Chalov, P.I. (1975) Isotopic fractionation of natural uranium (*in Russian*). Frunze, «Ilim».

515 Cherniak, D.J., and Pyle, J.M. (2008) Th diffusion in monazite. Chemical Geology, 256, 52-61.

516 Dubinchuk, V.T., and Sidorenko, G.A. (1978) On forms of lead entrainment into natural oxides
517 of uranium (*in Russian*). Geokhimia, 1, 96-101.

518 Eyal, Y., and Fleischer, R.L. (1985a) Timescale of natural annealing in radioactive minerals
519 affects retardation of radiation-damage-induced leaching. Nature, 314, 518-520.

520 Eyal, Y., and Fleischer, R.L. (1985b) Preferential leaching and the age of radiation damage from
521 alpha decay in minerals. Geochimica et Cosmochimica Acta, 49, 1155-1164.

522 Gieré, R., Swope, R.J., Buck, E.C., Guggenheim, R., Mathys, D., and Reusser, E. (2000) Growth
523 and alteration of uranium-rich microlite. Materials Research Society, Symposium
524 Proceedings, 608, 519-524.

525 Gieré, R., Hatcher, C., Reusser, E., and Buck, E.C. (2002) Element partitioning in pyrochlore-
526 based ceramic nuclear waste form. Materials Research Society, Symposium Proceedings,
527 713, 303-311.

528 Gieré, R., Williams, C.T., Wirth, R., and Ruschel, K. (2009) Metamict fergusonite-(Y) in
529 spessartine-bearing granitic pegmatite from Adamello, Italy. Chemical Geology, 261, 333-
530 345.

531 Hawthorne, F.C., Groat, L.A., Raudsepp, M., Ball, N.A., Kimata, M., Spike, F.D., Gaba, R.,
532 Halden, N.M., Lumpkin, G.R., Ewing, R.C., Greegor, R.B., Lytle, F.W., Ercit, T.S.,
533 Rossmann, G.R., Wicks, F.J., Ramik, R.A., Sherriff, B.L., Fleet, M.E., McCammon, C.
534 (1991) Alpha-decay damage in titanite. American Mineralogist, 76, 370-396.

Icenhower, J.P., McGrail, B.P., Schaef, H.T., and Rodriguez, E.A. (2000) Dissolution kinetics of titanium pyrochlore ceramics at 90 °C by single-pass flow-through experiments. Materials Research Society, Symposium Proceedings, 608, 373-378.

Kramers, J., Frei, R., Newville, M., Kober, B., and Villa, I. (2009) On the valency state of radiogenic lead in zircon and its consequences. Chemical Geology, 261, 4-11.

Krivitsky, A.G., Batrakov Yu.F., Bogdanov, R.V., and Puchkova, E.V. (2004) An X-ray spectroscopy approach to interpretation of valency of heavy atoms as exemplified by uranium in its UO_{2+x} oxides (*in Russian*). Proc. of the III Scientific Session of the Chemistry Centre of St. Petersburg State University, Saint Petersburg, 87-89.

Krivitsky, A.G., Bogdanov, R.V., and Batrakov, Yu.F. (2004) Chemical shift and widening of the $UL\gamma_6$-line as parameters for identifying the chemical state of the uranium atom. *In:* Qaim, S.M., and Coenen, H.H. (eds) Advances in Nuclear and Radiochemistry. 6th International Conference on Nuclear and Radiochemistry. Aachen, Germany, Extended Abstracts, 3, 92-94.

Komarov, A.N. (1977) On species of uranium in some minerals used for U-Pb dating (*in Russian*) In Collection: Dating Problems of Precambrian Formations. Leningrad: "Nauka" L/O, 225 -234.

Komarov, A.N., Makeev, A.F., Levchenkov, O.A., Ganzey, S.S., and Bubnova, R.C. (1980) Studies of thermal history of some minerals based on integrity of radiation-induced damage for geochronology purposes (*in Russian*). Proc. Academy of Sciences, USSR, Geology Series, 1, 47-53.

Komarov, A.N., Berman, I.B., and Koltsova, T.V. (1985) Radiography-based distribution of uranium and thorium in some granulites *(in Russian)*. Geokhimia, 7, 979-987.

558 Kudryashov, N.M., Lyalina, L.M., and Apanasevich, E.A. (2015) Age of rare-metal pegmatites
559 from the Vasin-Myl'k deposit (Kola region): Evidence from U-Pb geochronology of
560 microlite. Doklady Earth Sciences, 461, Part 2, 321-325.
561 Lumpkin, G.R., Foltyn, E.M., and Ewing, R.C. (1986) Thermal recrystallization of alpha-recoil
562 damaged minerals of the pyrochlore structure type. Journal of Nuclear Materials, 139, 113-
563 120.
564 Lumpkin, G.R., and Ewing, R.C. (1988) Alpha-decay damage in minerals of the pyrochlore
565 group. Physics and Chemistry of Minerals, 16, 2-20.
566 Lumpkin, G.R., Day, R.A., McGlinn, P.J., Payne, T.E., Gieré, R., Williams, C.T. (1999)
567 Investigation of the long-term performance of betafite and zirconolite in hydrothermal veins
568 from Adamello, Italy. Materials Research Society, Symposium Proceedings, 556, 793-801.
569 Lumpkin, G.R. (2001) Alpha-decay damage and aqueous durability of actinide host phases in
570 natural systems. Journal of Nuclear Materials, 289, 136-166.
571 Lumpkin, G.R., Gao, Y., Gieré, R., Williams, C.T., Mariano, A.N., and Geisler, T. (2014) The
572 role of Th-U minerals in assessing the performance of nuclear waste forms. Mineralogical
573 Magazine 78, 1071-1096.
574 Lutze, W., and Ewing, R.C. (eds) (1988) Radioactive Waste Forms for the Future. Elsevier
575 Science Publishers B. V., North-Holland Physics, Amsterdam.
576 Meldrum, A., Boatner, L.A., Weber, W.J., and Ewing, R.C. (1998) Radiation damage in zircon
577 and monazite. Geochimica et Cosmochimica Acta, 62, 2509-2520.
578 Olander, D.R., and Eyal, Y. (1990) Leaching of uranium and thorium from monazite: II.
579 Elemental leaching. Geochimica et Cosmochimica Acta, 54, 1879-1887.

Orlova, A.I., Orlova, V.A., Orlova, M.P., Bykov, D.M., Stephanovsky, S.V., Stephanovskaya, O.I., and Nikonov, B.S. (2006) A crystallochemical principle in design of mineral-like phosphate ceramics for the immobilization of radioactive wastes (*in Russian*). Radiokhimia, 48/4, 297-304.

Salje, E.K.H., Safarik, D.J., Taylor, R.D., Pasternak, M.P., Modic, K.A., Groat L.A., and Lashley J.C. (2011) Determination of iron sites and the amount of amorphization in radiation-damaged titanite ($CaSiTiO_5$). Journal of Physics: Condensed Matter, 23, 10, 105402-105404.

Schlenz, H., Heuser, J., Neumann, A., Schmitz, S., and Bosbach, D. (2013) Monazite as suitable actinide waste form. Zeitschrift für Kristallographie – Crystalline Materials, 228/3,113-123.

Seydoux-Guillaume, A.-M., Montel, J.-M., Bingen, B., Bosse, V., de Parseval, Ph., Paquette, J.-L., Janots, E., Wirth, R. (2012) Low-temperature alteration of monazite: Fluid mediated coupled dissolution-precipitation, irradiation damage, and disturbance of the U-Pb and Th-Pb chronometers. Chemical Geology, 330/331, 140-158.

Shirvington, P.J. (1983) Fixation of radionuclides in the ^{238}U decay series in the vicinity of mineralized zones: 1. The Austatom Uranium Prospect, Northern Territory, Australia. Geochimica et Cosmochimica Acta, 47, 403-412.

Stefanovsky, S.V., Yudintsev, S.V., Gieré, R., and Lumpkin, G.R. (2004) Nuclear waste forms. *In:* Gieré, R., and Stille, P. (eds) Energy, Waste, and the Environment: a Geochemical Perspective. Geological Society, London, Special Publications 236, 37-63.

Strachan, D.M., Scheele, R.D., Buck, E.C., Icenhower, J.P., Kozelisky, A.E., Sell, R.L., Elovich, R.J., and Buchmiller, W.C. (2005) Radiation damage effects in candidate titanates for Pu disposition: Pyrochlore. Journal of Nuclear Materials, 345, 109-135.

603 Tsimbal, L.F., Naumov, G.B., Maksimova, I.G., and Danilchenko, A.Ya. (1986) To the
604 technique of qualitative analysis of uranium species in rocks (*in Russian*), Geokhimia, 4,
605 502-511.
606 Tugarinov, A.I., Bibikova, E.V., Grachev, T.V., and Makarov, V.A. (1974) On the
607 geochronology of the White Sea formation. *In*: New data on the absolute geochronology (*in*
608 *Russian*). Nauka, Moscow, p. 120-124.
609 Volkov, Yu.F. (1999) Compounds with zircon and monazite structure and possibility of their use
610 for the inclusion of radionuclides (*in Russian*). Radiokhimia, 41/2, 161-166.
611 Vorobi'ev, Yu.K. (1990) Regularities of growth and evolution of mineral crystals (*in Russian*).
612 Nauka, Moscow, pp.184
613 Weigel, F. (1986) Uranium. *In:* Katz, J.J., Seaborg, G.T., Morss, L.R. (eds) The Chemistry of the
614 Actinide Elements, Vol. 1, 2nd Edition. London, New York, Chapman and Hall, 186-460.
615 Zhang, M., Salje, E. K.H., and Ewing, R.C. (2002) Infrared spectra of Si-O overtones, hydrous
616 species, and U ions in metamict zircon: radiation damage and recrystallization. Journal of
617 Physics: Condensed Matter, 14/12, 3333-3352.
618 Zhang, M., Salje, E. K.H., and Ewing, R.C. (2003) Oxidation state of uranium in metamict and
619 annealed zircon: near-infrared spectroscopic quantitative analysis. Journal of Physics:
620 Condensed Matter, 15/20, 3445-3470.
621 Zhang, Y., Zhang, Z., Thorogood, G., and Vance, E.R. (2013) Pyrochlore based glass-ceramics
622 for the immobilization of actinide-rich nuclear wastes: From concept to reality. Journal of
623 Nuclear Materials, 432/1-3, 545-547.
624
625
626
627

This is a preprint, the final version is subject to change, of the American Mineralogist (MSA)
Cite as Authors (Year) Title. American Mineralogist, in press.
(DOI will not work until issue is live.) DOI: http://dx.doi.org/10.2138/am-2016-5475

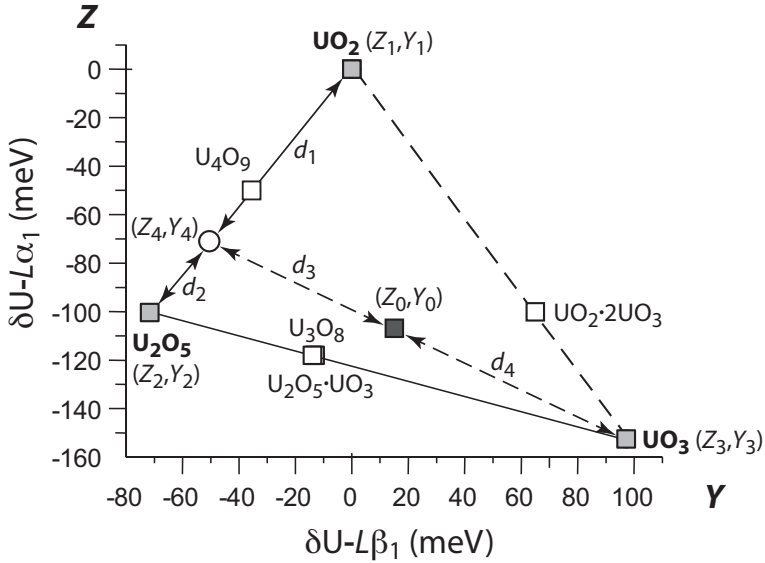

Figure 1. Correlation diagram of the chemical shifts δ for the *L*α1 and *L*β1 X-ray emission lines of uranium in compounds of the composition UO_{2+X} ($X = 0 - 1$). See text for discussion.

This is a preprint, the final version is subject to change, of the American Mineralogist (MSA)
Cite as Authors (Year) Title. American Mineralogist, in press.
(DOI will not work until issue is live.) DOI: http://dx.doi.org/10.2138/am-2016-5475

Table 1. Redox forms of uranium in the studied minerals, as determined by the data obtained from the X-ray spectral studies

Sample	Chemical Shift δ (meV)		Relative line broadening ΔΓ (meV)		Relative content (%)			Oxygen coefficient in the oxide UO_{2+X}
	δU-$L\alpha_1$	δU-$L\beta_1$	ΔΓU-$L\alpha_1$	ΔΓU-$L\beta_1$	U^{4+}	U^{5+}	U^{6+}	
Microlite 1	-86±5	+34±7	+41±24	-176±48	34.2	17.6	48.2	$UO_{2.570}$
Microlite 2	-89±5	+22±6	+54±24	-157±46	32.0	26.0	42.0	$UO_{2.550}$
Monazite 1	-38±7	+19±14	+59±42	-670±81	73.7	3.8	22.5	$UO_{2.244}$
Monazite 2	-28±8	-12±12	-21±48	-478±61	74.2	21.9	3.9	$UO_{2.149}$

This is a preprint, the final version is subject to change, of the American Mineralogist (MSA)
Cite as Authors (Year) Title. American Mineralogist, in press.
(DOI will not work until issue is live.) DOI: http://dx.doi.org/10.2138/am-2016-5475

Table 2. Isotopic composition of uranium in hydrochloric acid leachates of monazite and xenotime

Mineral and composition of the solution	**Activity Ratio (= $^{234}U/^{238}U$)** (Bq/Bq)			**Content of $^{238}U^{4+}$ in leachates (%)**
	U^{4+}	U^{6+}	ΣU	
Monazite #9 6 mol/L HCl + 0.6 mol/L $C_2H_8O_6$	0.94±0.02	0.81±0.04	0.92±0.03	90 ± 5
Monazite #10 6 mol/L HCl + 0.6 mol/L $C_2H_8O_6$	0.97±0.01	0.96 ±0.01	0.97 ±0.01	63 ± 12
Monazite #10 6 mol/L HCl + 0.6 mol/L $NH_2OH \cdot HCl$	0.97±0.01	0.97±0.01	0.97±0.01	–
Monazite #10 6 mol/L HCl (no reducing agent)	0.965±0.005	0.997±0.005	0.979±0.005	59 ± 12
Xenotime 6 mol/L HCl + 0.6 mol/L $C_2H_8O_6$	0.93±0.04	0.98±0.02	0.94±0.04	82 ± 8
Monazite (data from Chalov, 1975)	0.92±0.02	0.93±0.02	0.93±0.02	97